Advances and Applications in Fluid Mechanics
Volume 2, Issue 1, 2007, Pages 59-70
This paper is available online at http://www.pphmj.com
© 2007 Pushpa Publishing House

FILM THICKNESS FOR TWO PHASE FLOW IN A MICROCHANNEL

RONAN GRIMES, COLIN KING and EDMOND WALSH

Stokes Research Institute
University of Limerick, Limerick, Ireland
e-mail: ronan.grimes@ul.ie

Abstract

The issue of contamination of micro channel surfaces by bio fluids is a significant impediment to the development of many biomedical devices. A solution to this problem is the use of a carrier fluid, which segments the bio fluid and forms a thin film between the bio fluid and the channel wall. A number of issues need to be addressed for the successful implementation of such a solution. Amongst these is the prediction of the thickness of the film of carrier fluid which forms between the bio sample and the channel wall. The Bretherton and Taylor laws relate the capillary number to the thickness of this film. This paper investigates the validity of these laws through an extensive experimental program in which a number of potential carrier fluids were used to segment aqueous droplets over a range of flow rates. The aqueous plugs were imaged using a high speed camera and their velocities were measured. Film thicknesses were calculated from the ratio of the velocity of the carrier fluid to the velocity of the aqueous plug. The paper concludes that significant discrepancies exist between measured film thicknesses and those predicted by the Bretherton and Taylor laws, and that when plotted against capillary number, film thickness data for the fluids collapsed onto separate curves. By multiplying the capillary number by the ratio of droplet to carrier fluid viscosity, the data for the different fluids collapsed onto a single curve.

www.pphmj.com

2000 Mathematics Subject Classification: 76-05.

Keywords and phrases: film thickness, two phase flow, micro fluidics, carrier fluid.

Communicated by Shahrdad G. Sajjadi.

Received February 22, 2007

Nomenclature

Symbol	Description	Unit
Ca	Capillary number	-
h	Film thickness	m
R	Channel radius	m
R_d	Droplet radius	m
$\overline{U}$	Mean channel velocity	m/s
U_d	Droplet velocity	m/s
μ	Carrier fluid viscosity	Pa s
σ	Water/carrier fluid interfacial tension	N/m

1. Introduction

The use of the Polymerase Chain Reaction (PCR) to exponentially amplify target DNA segments has found widespread applications in a diversity of fields, ranging from molecular diagnostics to forensic science. The reaction involves the thermal cycling of reagents through temperatures of typically 95 to 55 to 72°C. Each thermal cycle doubles the quantity of DNA present. The cycle was conventionally performed in relatively large scale stationary wells. This had a number of drawbacks, including large thermal mass and therefore long cycle times, the requirement for large volumes of expensive reagents, and low throughput. As a solution to these issues micro scale flowing PCR reactors were developed.

www.pphmj.com

Since the inception of micro scale PCR it was recognised that surface chemistry would play an important role due to the inherent high surface to volume ratios (Cheng and Kricka, [5]). The problem was noted by a number of investigators. Wilding et al. [16] and Shoffner et al. [14] identified that contact between PCR samples and silicon channels made PCR difficult to achieve. Panaro et al. [11] quantified the effects of channel surface absorption for a number of typical micro channel materials. This investigation concluded that contact between the PCR

sample and the majority of the material surfaces tested either reduced the efficiency or completely inhibited PCR. Park et al. [12] observed similar problems for fused silica capillaries. Auroux et al. [1] stated that the greatest problem with micro scale PCR is the elevated absorption of the reaction components onto surfaces as a result of the high surface to volume ratios. It is therefore clear that a solution to the issue of absorption is necessary for reliable and reproducible micro scale PCR to become a reality.

Panaro et al. [11] and Park et al. [12] amongst others have described surface treatment procedures which may be used to overcome such problems. However these procedures tend to be time consuming, and their success has been shown to be limited. According to Auroux et al. [1] surface coating procedures such as silinization are possible, but may lack reproducibility.

An alternative solution which was proposed by Dorfman et al. [6] was the use of a carrier fluid which is immiscible with the PCR sample, and which forms a film between the PCR sample and the channel wall. This film acts as a barrier to the absorption of bio molecules from the PCR sample to the solid surface. Successful, contamination free PCR was demonstrated using this approach. The carrier fluid used by Dorfman et al. was FC-40 Fluorinert Fluid. Walsh et al. [15] have shown a number of other fluids including tetradecane, mineral oil, dodecane and silicone oil to be PCR compatible by bringing the PCR sample into contact with the carrier fluid in a stationary well and subsequently thermally cycling the PCR sample.

www.pnrmi.com

Whilst the carrier fluids listed above have been shown to be compatible with the PCR when the interaction is static, many questions remain unanswered from a fluid dynamics perspective. One such issue is the thickness of the film of carrier fluid between the PCR sample and the channel wall. If the film is too thin, then asperities in the wall can protrude through the carrier fluid film and make contact with the PCR sample. Contamination of such asperities can transfer to subsequent droplets, resulting in cross contamination. Droplet break-up can also result from contact between such an asperity and a droplet.

For low capillary numbers, the relationship between film thickness, tube radius and capillary number is given by the Bretherton law (Aussillous and Quere, [2]):

$$h/R = 1.34Ca^{2/3}, \tag{1}$$

where

$$Ca = \frac{\mu\overline{U}}{\sigma}. \tag{2}$$

Aussillous and Quere [2] suggest that for higher values of the capillary number Taylor's Law, rather than Bretherton's law should be used:

$$\frac{h}{r} = \frac{1.34Ca^{2/3}}{1 + 3.35Ca^{2/3}}. \tag{3}$$

Aussillous and Quere [2] further suggest that a threshold Capillary number exists, beyond which film thicknesses are in excess of those predicted by Taylor's Law. This threshold capillary number, Ca^* is given by equation 4.

$$Ca^* = \left(\frac{\mu}{\sigma\rho R}\right)^{3/4}. \tag{4}$$

Experimental data was presented by Aussillous and Quere [2] which support these equations. However, the data was recorded for air bubbles in liquid carrier fluids, and as a result the carrier to droplet fluid viscosity ration was extremely high relative to those typical of two phase liquid flows. This paper investigates the validity of the Taylor and Bretherton laws in predicting film thickness for a range of capillary numbers and viscosity ratios typical of those which might be found in PCR reactors. The paper concludes that these laws are inaccurate in predicting film thickness when droplet viscosity is of similar magnitude to carrier fluid viscosity. Furthermore, it is shown that when plotted against capillary number, film thickness values for the fluids investigated do not collapse onto a single curve as has been reported in literature for liquid/gas two phase flows. However, when the capillary number was multiplied by the ratio of droplet to carrier fluid viscosity, the data for all the carrier fluids collapses onto a single curve.

www.pphmj.com

Experimentation

The experimental configuration which was used is illustrated in Figure 1. A 5 ml Hamilton gastight syringe was mounted on to a Harvard Apparatus PHD 2000 syringe pump. This syringe was filled with the carrier fluid and connected using Upchurch fittings to Teflon tubing with an internal diameter of 0.762 mm, and external diameter of 1.6 mm. At the start of each experiment, the tube was filled with the carrier fluid from the syringe and a volume of distilled water was loaded into the tube from an eppendorf filled with distilled water and the carrier fluid. The resulting plug was measured to be 1mm±0.02mm long when static in the tube. The free end of the tubing was then inserted into a reservoir of carrier fluid. The plug was then pumped to the syringe end of the tubing from where it was started for each experimental measurement. The distance between the start point and the first viewpoint in the tubing was approximately 360 mm. The syringe was then programmed to dispense carrier fluid at the necessary flow rate to give the required mean velocity in the tube. The water droplet was thus displaced along the length of the tube.

The droplet was imaged using an IDT X-Stream™ XS-4 CMOS high speed camera mounted on an Olympus IX50 microscope. The portion of the tubing which was imaged was immersed in water, in a transparent bath. This reduced the effects of refractive index mismatches, and allowed the droplets to be viewed more clearly. As illustrated in Figure 1, the tubing was looped around so that the plug passed through the viewing window twice. The length of tubing between the two imaging points was approximately 570 mm. Knowing the distance between these two points, it was possible to calculate the velocity of a plug, by measuring the time interval between the first and second pass of the droplet through the imaging point.

www.pphmj.com

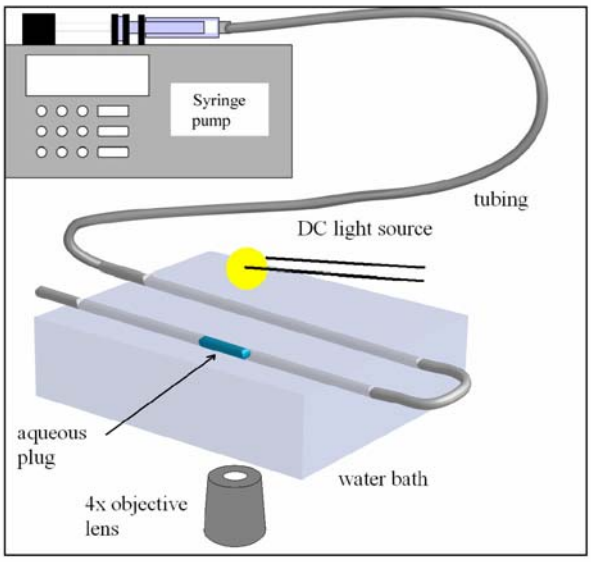

Figure 1. Schematic of experimental set up.

The carrier fluids tested were FC-40 Fluorinert Fluid supplied by Acota, with the addition of 0.75wt.% 1H, 1H, 2H, 2H-Perfluorodecan-1-o1 surfactant supplied by Fluorochem, Dodecane (44030) supplied by Sigma-Aldrich and Tetradecane (172456) supplied by Sigma Aldrich. Viscosity and interfacial tensions are listed in Table 1 for each of these fluids. Also listed in Table 1 is the viscosity to interfacial tension ratio of each of the fluids. For a given fluid velocity the Capillary number is directly proportional to this value. Tests were carried out with mean capillary velocities ranging from 0.5×10^{-3} m/s to 400×10^{-3} m/s.

www.pphmj.com

Table 1. Properties of carrier fluids tested

	μ(Pas)	σ(N/m)	μ/σ(s/m)
FC-40	0.0034 (Dorfman et al. [6])	0.019 (3M [17])	0.18
Tetradecane	0.0019 (Alexandre et al. [13])	0.044 (Garti et al. [7])	0.045
Dodecane	0.0013 (Caudwell et al. [4])	0.052 (Hool et al. [8])	0.026

As it was not possible to completely eliminate the effects of refractive index mismatch, a direct measure of film thickness could not be obtained from the recorded images. Therefore, an indirect method of film thickness measurement was employed. The presence of the film causes the droplet to be displaced at a higher velocity than the mean flow velocity. The ratio of droplet velocity to mean flow velocity can be related to the droplet radius and hence film thickness using equation 4 (Kashid et al. [9]). The droplet velocity U_d was measured using the imaging technique described above, whilst the mean velocity U was calculated from the flow rate set on the syringe pump and the known cross sectional area of the tubing.

$$U_d = \frac{2}{1 + (R_d/R)^2} \overline{U}. \tag{5}$$

Results and Discussion

In this section the experimental results are presented. Firstly the droplet images are introduced for each of the carrier fluids for a range of capillary numbers. Film thicknesses versus capillary numbers are then plotted for each of the carrier fluids and the measured values are compared with those predicted by the Bretherton and Taylor laws.

Figure 2 shows the development in droplet shape with increasing capillary number for all the carrier fluids tested. The common trend amongst all the carrier fluids is the change in shape of the droplet from a cylinder with hemispherical ends at low capillary numbers, to an elongated bullet like shape, with a flattened trailing edge, and tapered leading edge at higher capillary numbers. This trend was reported by Olbricht and Kung [10] for other fluids. It can be seen that at low velocities the film thickness is small. This can cause the droplet to interact with any asperities present in the tubing, which in turn can cause droplet breakup and the formation of satellite droplets as reported by Dorfman et al. [6]. It is apparent from the pictures that this is not an issue for the range of velocities and fluids tested here. At higher capillary numbers Olbricht and Kung [10] reported instabilities caused by extreme deformation of the droplet. The onset of such a high capillary number instability is evident for FC-40 at 400mm/s. This is indicative of an upper

www.pprmj.com

limit on velocity, which can be achieved with an aqueous droplet in a FC-40 carrier fluid. No instability of this type was evident for either of the other fluids investigated, their capillary numbers being significantly lower.

Figure 3 shows the variation in film thickness with capillary number for each of the fluids tested. As one would expect, the general trend is an increase in film thickness with increased capillary number. Also apparent is the significant discrepancy between the measured film thickness and the film thickness calculated from the Bretherton Law of equation 1 and Taylor Law of equation 3.

Table 2 presents the threshold capillary number given by equation 4 for each of the fluids. Aussillous and Quere [2] suggest that below this Capillary number, the film thickness should be predicted by the Taylor Law, and above these values the film thickness should be in excess of Taylor's Law predictions. However it can be seen that the threshold capillary numbers are in excess of the capillary numbers obtained in these experiments. Despite this the film thicknesses for all fluids are in excess of Taylor's Law predictions. It should also be noted that data for each of the fluid collapses onto separate curves.

www.pphmj.com

Table 2. Threshold capillary number for carrier fluids tested

	Ca^*
FC-40	0.35
Tetradecane	0.24
Dodecane	0.16

In Figure 4 the capillary number is multiplied by the ratio of water to carrier fluid viscosity. This causes the data for all the carrier fluids to collapse onto a single curve. Previous authors have reported that when plotted against capillary number, film thickness data should collapse onto a single curve, as suggested by the Bretherton and Taylor laws. However, these investigations were performed for two phase liquid gas flows, where the viscosity of the gas was orders of magnitude lower than that of the

liquid. To the knowledge of the authors this is the first time film thickness has been observed to collapse as illustrated in Figure 4, and it is likely to be a result of the fluid viscosities being of similar magnitudes.

Conclusions

- Qualitatively, the variation in shape of the droplets with increased capillary number followed similar trends to those observed by past investigators.
- For all the fluids, film thickness was sufficient to prevent channel wall asperities from creating satellite droplets at low capillary numbers.
- The onset of a high capillary number instability was observed for FC-40 at a velocity of 400mm/s, indicating the velocity limit for an aqueous droplet in this carrier fluid.
- Significant discrepancies were observed between measured film thicknesses and those predicted by the Bretherton and Taylor laws.
- When plotted against capillary number, film thickness values for the three fluids tested collapse onto three separate curves.
- When plotted against the product of capillary number and the ratio of droplet to carrier fluid viscosity, the film thickness data for the three fluids test collapsed onto a single curve.

www.ipimj.com

Acknowledgements

The authors of this paper would like to acknowledge the support of Enterprise Ireland through the Basic Research Grant Scheme.

References

[1] P.-A. Auroux, Y. Koc, A. deMello, A. Manz and P. J. R. Day, Miniaturised nucleic acid analysis, Lab Chip 4 (2004), 534-546.

[2] P. Aussillous, and D. Quere, Quick deposition of a fluid on the wall of a tube, Phys. Fluids 12(10) (2000), 2367-2371.

[3] J. Bico and D. Quere, Liquid trains in a tube, Europhysics Letters 51(5) (2000), 546-550.

[4] D. R. Caudwell, J. P. M. Trusler, V. Vesovic and W. A. Wakeham, The viscosity and density of n-dodecane and n-octadecane at pressures up to 200 MPa and temperatures up to 473 K, Fifteenth Symposium on Thermophysical Properties, Boulder, CO, USA, June 22-27, 2003.

[5] J. Cheng and L. J. Kricka, Biochip Technology, Harwook Academic Publishers, 2001.

[6] K. D. Dorfman, M. Chabert, J.-H. Codarbox, G. Rousseau, P. de Cremoux and J.-L. Viovy, Contamination-free continuous flow microfluidic polymerase chain reaction for quantitative and clinical applications, Anal. Chem. 77(11) (2005), 3700-3704.

[7] N. Garti, A. Benichou and A. Aserin, Steroid-saponins from fenugreek seeds as emulsifier, foaming agents and anticholesterol agents-extraction, purification, and surface properties.
(http://www.yissum.co.il/admin/project/project_preview.asp?ind=115)

[8] K. Hool and B. Schuchardt, A new instrument for the measurement of liquid-liquid interfacial tension and the dynamics of interfacial tension reduction, Meas. Sci. Technol. 3 (1992), 451-457.

[9] M. N. Kashid, I. Gerlach, S. Goetz, J. Franzke, J. F. Acker, F. Platte, D. W. Agar and S. Turek, Internal circulation within the liquid slugs of a liquid-liquid slug-flow capillary microreactor, Ind. Eng. Chem. Res. 44 (2005), 5003-5010.

[10] W. L. Olbricht and D. M. Kung, The deformation and breakup of liquid drops in low Reynolds number flow through a capillary, Phys. Fluids A 4 (7) (1992), 1347-1354.

[11] N. J. Panaro, X. J. Lou, P. Fortina, L. J. Krick and P. Wilding, Surface effects on PCR reactions in multichip microfluidic platforms, Biomedical Microdevices 6(1) (2004), 75-80.

[12] N. Park, S. Kim and J. H. Hahn, Cylindrical compact thermal-cycling device for continuous-flow polymerase chain reaction, Anal. Chem. 75 (2003), 6029-6033.

[13] Alexandre I. Romoscanu, M. B. Sayir, K. Häusler and C. Servais, High frequency probe for the measurement of the complex viscosity of liquids, Meas. Sci. Technol. 14 (2003), 451-462.

[14] M. A. Shoffner, J. Cheng, G. E. Hvichia, L. J. Kricka and P. Wilding, Chip PCR. I. Surface passivation of microfabricated silicon-glass chips for PCR, Nucl. Acids Res. 24 (1996), 375-379.

[15] E. Walsh, C. King, R. Grimes and A. Gonzalez, Segmenting fluid effect on PCR reactions in microfluidic platforms, Biomedical Microdevices 7(4) (2005), 269-272.

[16] P. Wilding, M. A. Shoffner, J. Cheng, G. E. Hvichia and L. J. Krika, Thermal cycling and surface passivation of micromachined devices for PCR, Clin. Chem. 41 (1995), 1367-1368.

[17] 3M, Thermal Management Fluids and Services, 2003.
http://multimedia.mmm.com/mws/mediawebserver.dyn?ddddddNLXpsdyHedrHeddd KDnP0DDDDC-.

www.pphmj.com

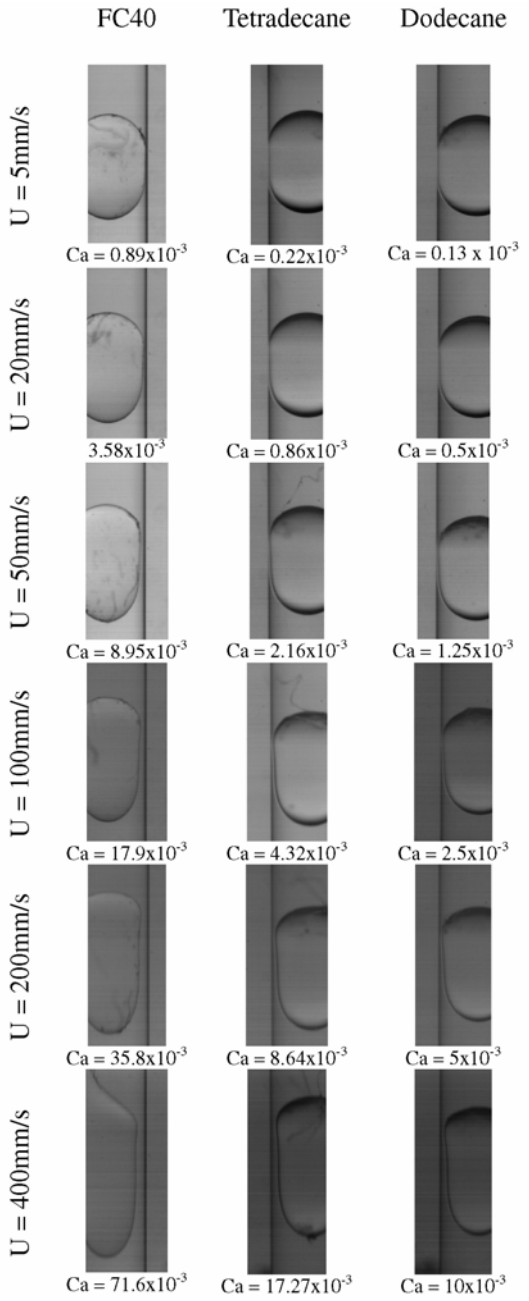

Figure 2. Visualisation of droplets for each of the carrier fluids tested over a range of mean velocities.

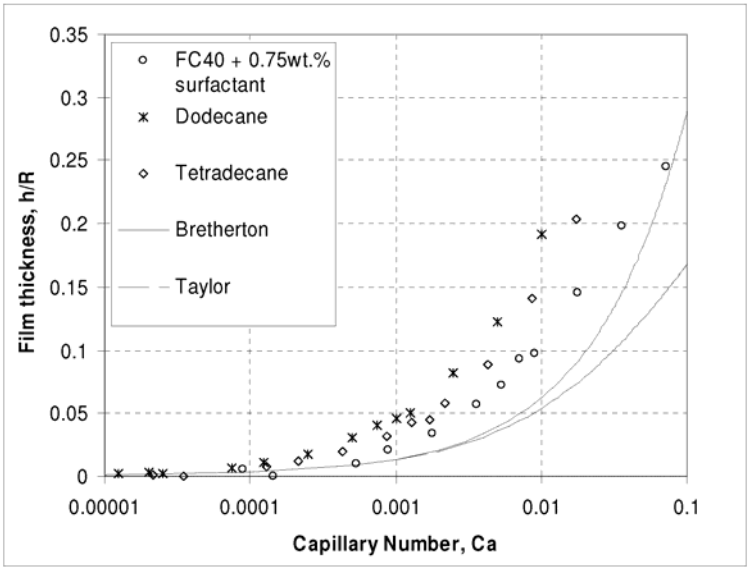

Figure 3. Measured film thickness for FC40, dodecane and tetradecane carrier fluids, and the Bretherton and Taylor Law predictions.

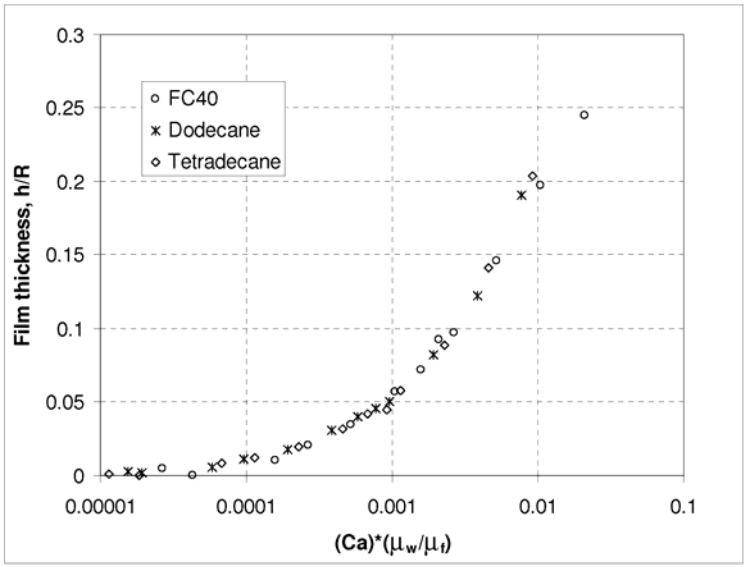

Figure 4. Measured film thickness for FC40, dodecane and tetradecane carrier fluids, plotted against the product of capillary number and viscosity ratio.